Electrochemistry Communications 12 (2010) 1062–1065

Contents lists available at ScienceDirect

Electrochemistry Communications

journal homepage: www.elsevier.com/locate/elecom

Facile fabrication of free-standing TiO_2 nanotube membranes with both ends open via self-detaching anodization

Jia Lin, Jingfei Chen, Xianfeng Chen *

Department of Physics; The State Key Laboratory on Fiber Optic Local Area Communication Networks and Advanced Optical Communication Systems, Shanghai Jiao Tong University, 800 Dongchuan Rd. Shanghai 200240, China

ARTICLE INFO

Article history:
Received 30 April 2010
Received in revised form 20 May 2010
Accepted 21 May 2010
Available online 27 May 2010

Keywords:
Anodic TiO_2 nanotubes
Membranes
Free-standing
Both ends open
Thermal stability

ABSTRACT

We report the first direct synthesis of free-standing TiO_2 nanotube membranes based on self-detaching electrochemical anodization. The films with high-quality surfaces and both-side-open tubes could be obtained by appropriate thermal treatment during the process. The membranes are optically transparent after subsequent annealing to induce crystallization. The possible mechanism of the multi-step electrochemical process is also presented. This self-detaching process developed here is easy and efficient without additional chemical dissolution or etching and is shown to open new prospects for the application of TiO_2 nanotubes in various fields.

1. Introduction

The exploitation of the unique properties and various applications of TiO_2 nanotubes holds great promise for the achievement of major breakthroughs in the fields of solar cells [1–3], photocatalytic degradation [4,5], water photoelectrolysis [6,7] and so on. Among various synthesis methods, electrochemical anodization has been demonstrated a facile and excellent approach to fabricate nanotube arrays, mostly on Ti foils. However, due to the underlying metal substrate, the feasibility for extensive applications has been restricted. In the back-side illuminated dye sensitized solar cells, inefficient illumination occurs [8]. Moreover, thermal treatments during crystallization result in an increase in the barrier layer thickness, non-ideal material crystallization and tube collapse due to oxide growth from the barrier layer [7,9]. The fabrication of transparent arrays on sputtered Ti was also investigated, though the procedures were complex and costly, which required special treatment of the metal layer in contact with the electrolyte surface [10] and strict process control [11]. The ability to obtain high-quality Ti films has remained a technological challenge [10,12], and the increase in film thickness will lead to the poor adhesion [13–15]. The advantages of free-standing nanotubes lie on their optimized microstructure, such as direct electrons transfer [2,10], and stability to mechanical vibrations [6,10]. It would also be more flexible of free-standing membranes for much wider applications, which can be directly used or attached onto foreign substrates [16–19]. Various techniques have been investigated for the synthesis of TiO_2 membranes, including ultrasonic splitting [18–20], solvent evaporation [16,21], selective metal dissolution [5,22] and chemically assisted delamination [1,2,23]. Due to the advantages of both-side-open tubes such as effective tube filling [19,24] and flow-through application [5], usually an additional chemical etching step was included to open the closed bottom end [4,5,19], and most recently a potential shock method was also reported [25]; for an overview see e.g. Ref. [26]. However, the widespread use of these techniques is somewhat limited as the approaches usually require delicate and complicated handling, and/or the preparation of free-standing arrays with optimal thicknesses for device applications is still a challenge.

In this present work, we introduce a new and effective technique with more handy experimental procedures, named 'self-detaching', for the synthesis of free-standing open-ended anodic nanotubes. TiO_2 layers were peeled off after a subsequent anodization among processing series without any other etchants, by taking the advantage of the different mechanical stability and marked etching contrast between the upper and lower layers. It is evident that the films feature high-quality surfaces and both-side-open tubes and this method would be generally applicable for the synthesis of membranes of various thicknesses. Our studies also have shown that better crystallinity could be obtained in free-standing membranes. The ability to fabricate these free-standing films is an essential step towards the exploitation of extended applications.

2. Experimental

In this work, a common two-electrode electrochemical cell was used with the working electrode Ti foil (0.2 mm thickness, Strem

* Corresponding author. Tel.: +86 2154743252.
E-mail address: xfchen@sjtu.edu.cn (X. Chen).

1388-2481/$ – see front matter © 2010 Elsevier B.V. All rights reserved.
doi:10.1016/j.elecom.2010.05.027

Chemicals) and the counter electrode Pt foil. Anodization was carried out in an ethylene glycol electrolyte containing 0.5 wt.% NH_4F + 3 vol.% deionized water under a constant voltage of 60 V. The time-dependent anodization current was measured using a sourcemeter (Keithley 2400). The anodization process was divided into three steps. For the first step, the Ti substrate was electrochemically pretreated using the solution for 0.5 h. After the first step, the as-formed TiO_2 layer was peeled off by intense ultrasonication in deionized water to expose the substrate. Surface-finished Ti were then subjected to the second anodization for 1–5 h and the resulting oxide layers were subjected to thermal treatments at 0–700 °C for 3 h. Afterwards, the as-formed films were completely detached by the third-step anodization under the same potentionstatic conditions for 0.5–1 h. The initial two steps were carried out at 10 °C and the third step at an elevated temperature of 30–50 °C. After anodization, the samples were annealed in order to obtain the crystalline phases of TiO_2. Field-emission scanning electron microscope (FE-SEM, FEI Sirion 200) was utilized for morphological and structural characterization. X-ray diffraction analysis (XRD, Rigaku D/Max-2200/PC, CuK_α) was performed for crystal phase identification.

3. Results and discussion

After the third step anodization at 30 °C for 1 h, the lift-off of the entire top layer (layer 1) was observed. During the detaching process, a new layer (layer 2) was formed underneath. The first two-step anodization resulted in nanoporous TiO_2 on the surface [27]. The tube length of layer 1 was around 10 μm (in 1 h) with the pore diameter around 100 nm (Fig. 1(a)), which can be precisely tailored by simply varying anodization parameters. For films thermal treated at 200 °C, although underwent etching during the self-detaching, few ruptures were observed on the top of the film, which is evident from Fig. 1(a). The tubular structure with a concave surface at the bottom side is evident from Fig. 1(b). Fig. 1(c) shows that there are numerous protrusions on the surface of layer 2. The match of the two surfaces implies that the nanotube arrays are disconnected at the interface between layer 1 and 2, resulting in open-ended tubes. Fig. 1(d) also presents the bottom of layer 2, which has the common hexagonal structure.

It can be clearly seen from Fig. 1(a′) and (b′) that tube bottom of films thermal treated at 400 °C is closed. The thin non-ordered compact oxide layer is present at the bottom of layer 1 and also partially at the

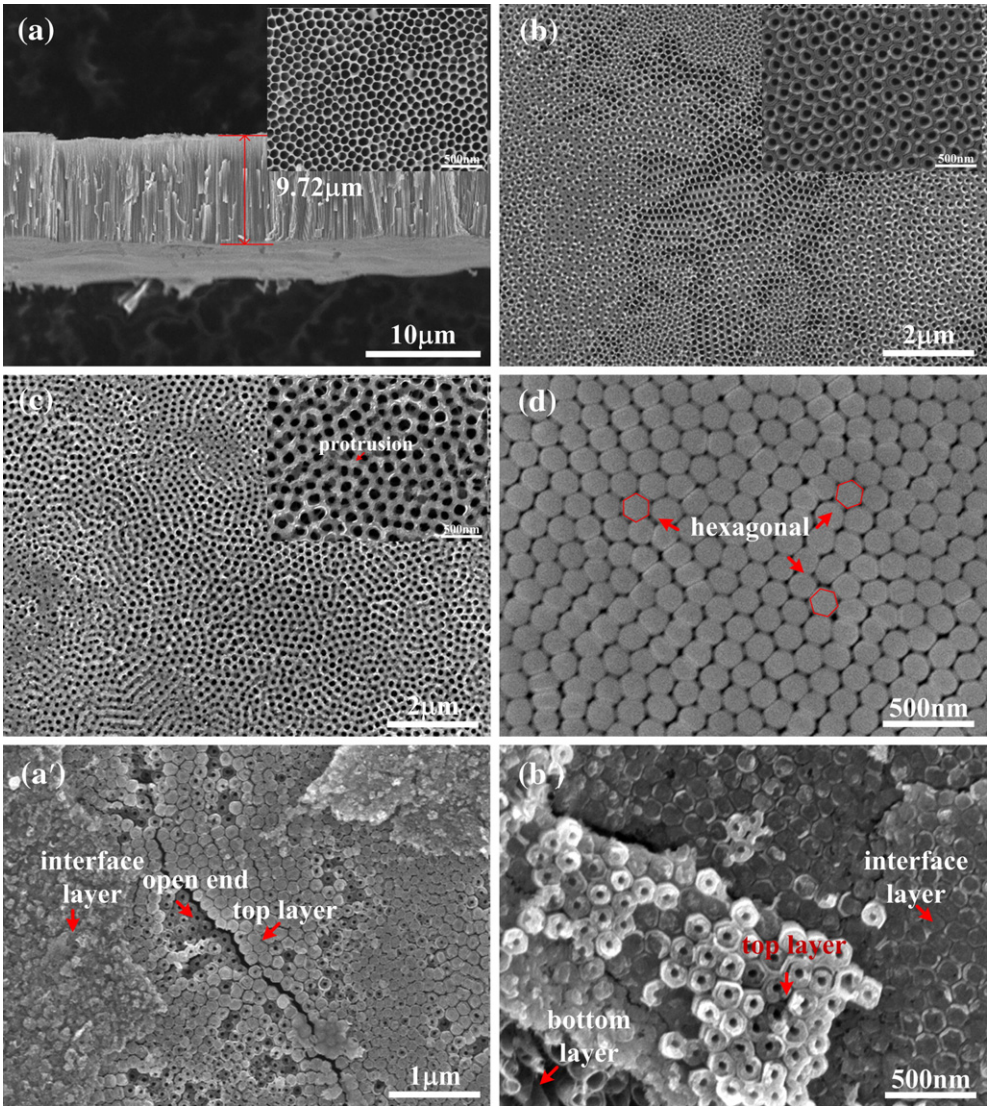

Fig. 1. FE-SEM images showing free-standing nanotube layers subjected to heat treatments at 200 (a–d) and 400 °C (a′, b′), respectively. (a) The thickness and top-view of layer 1. (b, c) The opening of the backside of layer 1 and the top-view of layer 2. The insets are the magnified view. (d) The bottom-view of layer 2. (a′) The closed-ended bottoms of layer 1. (b′) The top-view of layer 2.

surface of layer 2. A new layer was formed during the third step under the barrier layer (Fig. 1(b′)). However, if the as-anodized film was thermal treated at 100 °C, it could not be peeled off after extended anodization. In fact, the experimental results reveal that the temperature range around 200 °C seems to be the most suitable for efficient open-ended membrane fabrication.

Fig. 2(a) and (b) shows the optical images of the film with open-ended bottoms before and after annealing. It is clear that the as-formed films remained amorphous, which were then annealed to induce crystallization and to increase the transparency. The as-annealed crystallized membranes are optically transparent in the visible region. The samples thermal treated at 400 °C during the detaching process crystallized in the anatase phase, resulting in transparent films without subsequent annealing.

The self-detaching process for the films is illustrated in Fig. 2(a′). Samples subjected to low temperature anodization and post-heat treatment possess less impurity and defect, which reveal a greater compactness and higher stability against chemical dissolution [28]. (1) The bottom of tubes thermal treated at low temperature is amorphous structure, which can be penetrated during successive anodization. Thus, the two layers are disconnected and tubes with both ends open could be obtained. (2) The anatase crystals form at elevated temperatures, within the tube walls, the bottom and the tube-support interface region, which show high resistance to chemical etching. Thus, tubes cannot be formed at the bottom and the interface region, leaving the closed bottoms.

Meanwhile, the elevated bath temperature at the third step is also crucial for the films to be peeled off. The high temperature anodization with the decrement of viscosity as well as the increment in the current density leads to enhanced field assisted chemical etching at the bottom and local chemical dissolution is expected to be more significant for newly formed TiO_2 nanotubes with less dense walls at the interface. Thus, the weak interconnection between the two layers occurs. It is evident that the higher the temperature, the shorter the time for layer 1 to be peeled off. The detaching time is 1 h at 30 °C, while at 35 °C reduces to 0.5 h. However, higher temperature for step 3 was not suitable due to severe etching of the surface of layer 1. Thus, the different mechanical stability and etching contrast between the two layers give rise to the detaching process, enabling the fabrication of intact TiO_2 layer with the bottom open.

As shown in Fig. 2(b′), after thermal treatment at 200 °C, current recovery was observed for the third-step anodization. The initial local minimum (Lm) can be explained by the slow chemical penetration through the upper layers. Then, the current density gradually elevated before reaching a local maximum (LM). Compared with the current curve for thin film, it takes longer time for the current density to achieve relatively stable value for 5 h-anodized samples. For samples treated at 400 °C, the initial current density is much larger due to decreased surface resistance of anatase [29]. The barrier oxide is not compact enough to prevent the passage of ions under the subsequent anodization. Samples at 500–600 °C behave in a way similar to that of the 400 °C treated ones. When an annealing process was applied at 700 °C, weak current flow was present within a reasonable period of time, indicating that the tube structure collapsed and the formation of dense rutile crystallites, which could hardly be penetrated. For comparison, we included also the curve recorded for the second step anodization (marked by 'normal'). The magnitude of current is an indication of the rate of oxidation and the difference in current density originates from the different reaction processes during the anodization.

The free-standing films were subjected to high-temperature annealing in ambient at 600 °C for 3 h, then characterized by XRD to

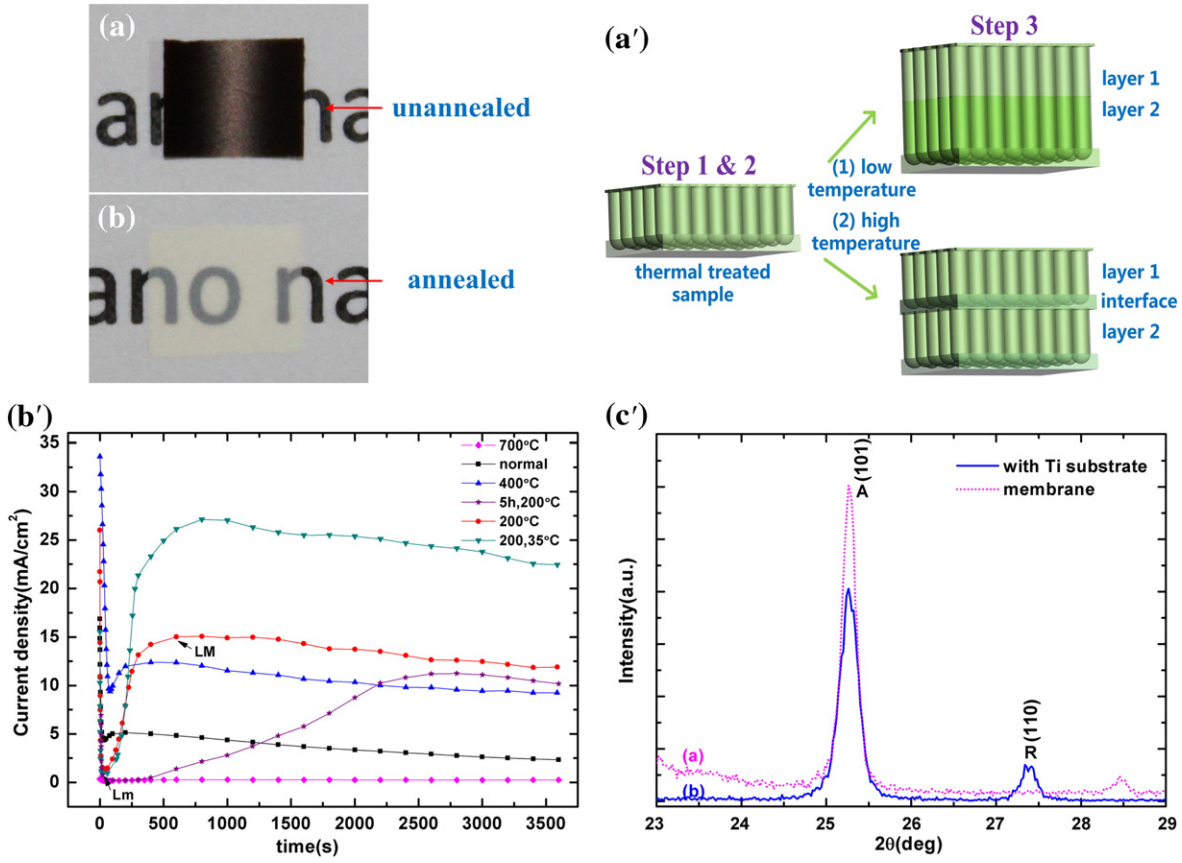

Fig. 2. (a, b) Optical images of samples thermal treated at 200 °C before and after annealing. (a′) Schematic representation of the formation of free-standing membranes by self-detaching anodization. (b′) The comparison of current-time behavior subjected to thermal treatment at different temperatures as indicated. (c′) XRD patterns of samples annealed at 600 °C in air for 3 h. A and R represent anatase and rutile, respectively.

confirm the crystalline phase. The crystallization behavior of nanotubes without the presence of Ti support is quite different. Fig. 2(c′) shows the XRD patterns of the films after annealing. Even after annealing of the free-standing membrane at 600 °C, the TiO_2 arrays consist only of the anatase crystal structure, which is evidenced from the diffraction peak at 25.3°. In contrast, for films on Ti support subjected to identical thermal treatment, both anatase and rutile peaks at 25.3° and 27.4°, respectively, were observed in the diffraction spectrum, indicating phase transformation from anatase to rutile crystal structure at the interface region at high temperature [30]. The enhanced crystallinity can be expected to improve the device performance through the reduction of defects and remaining amorphous regions.

4. Conclusions

In conclusion, a new approach based on the self-detaching anodization under potentiostatic conditions has been developed for the straightforward fabrication of free-standing TiO_2 membranes with tunable thickness and both ends open. The process consists of a common anodization followed by a thermal treatment and subsequent anodization. It is expected that such kind of self-detached TiO_2 nanofilms with both ends open and high crystallinity will have many potential applications in various fields.

Acknowledgments

This research was supported by the National Natural Science Foundation of China (10874119); the National Basic Research Program "973" of China (No. 2007CB307000); the Shanghai Leading Academic Discipline Project (B201); and Instrumental Analysis Center, Shanghai Jiao Tong University.

References

[1] J.H. Park, T.-W. Lee, M.G. Kang, Chem. Commun. 2008 (2008) 2867.
[2] Q.W. Chen, D.S. Xu, J. Phys. Chem. C 113 (2009) 6310.
[3] J.M. Macak, H. Tsuchiya, A. Ghicov, P. Schmuki, Electrochem. Commun. 7 (2005) 1133.
[4] S.P. Albu, A. Ghicov, J.M. Macak, R. Hahn, P. Schmuki, Nano Lett. 7 (2007) 1286.
[5] C.J. Lin, W.Y. Yu, Y.T. Lu, S.H. Chien, Chem. Commun. 2008 (2008) 6031.
[6] Y.B. Liu, B.X. Zhou, J. Bai, J.H. Li, J.L. Zhang, Q. Zheng, X.Y. Zhu, W.M. Cai, Appl. Catal. B 89 (2009) 142.
[7] K. Shankar, G.K. Mor, H.E. Prakasam, S. Yoriya, M. Paulose, O.K. Varghese, C.A. Grimes, Nanotechnology 18 (2007) 065707.
[8] K. Shankar, J. Bandara, M. Paulose, H. Wietasch, O.K. Varghese, G.K. Mor, T.J. LaTempa, M. Thelakkat, C.A. Grimes, Nano Lett. 8 (2008) 1654.
[9] O.K. Varghese, D.W. Gong, M. Paulose, C.A. Grimes, E.C. Dickey, J. Mater. Res. 18 (2003) 156.
[10] G.K. Mor, O.K. Varghese, M. Paulose, C.A. Grimes, Adv. Funct. Mater. 15 (2005) 1291.
[11] B.Y. Yu, A. Tsai, S.P. Tsai, K.T. Wong, Y. Yang, C.W. Chu, J.J. Shyue, Nanotechnology 19 (2008) 255202.
[12] A.Z. Sadek, H.D. Zheng, K. Latham, W. Wlodarski, K. Kalantar-zadeh, Langmuir 25 (2009) 509.
[13] M. Paulose, K. Shankar, O.K. Varghese, G.K. Mor, C.A. Grimes, J. Phys. D: Appl. Phys. 39 (2006) 2498.
[14] H.D. Zheng, A.Z. Sadek, M. Breedon, D. Yao, K. Latham, J.D. Plessis, K. Kalantar-Zadeh, Electrochem. Commun. 11 (2009) 1308.
[15] O.K. Varghese, M. Paulose, C.A. Grimes, Nature Nanotechnology 4 (2009) 592.
[16] H. Park, W.R. Kim, H.T. Jeong, J.J. Lee, H.G. Kim, W.Y. Choi, Sol. Energy Mater. Sol. Cells, in press.
[17] T.S. Kang, A.P. Smith, B.E. Taylor, M.F. Durstock, Nano Lett. 9 (2009) 601.
[18] Q.W. Chen, D.S. Xu, Z.Y. Wu, Z.F. Liu, Nanotechnology 19 (2008) 365708.
[19] D. Fang, K.L. Huang, S.Q. Liu, D.Y. Qin, Electrochem. Commun. 11 (2009) 901.
[20] M. Paulose, H.E. Prakasam, O.K. Varghese, L. Peng, K.C. Popat, G.K. Mor, T.A. Desai, C.A. Grimes, J. Phys. Chem. C 111 (2007) 14992.
[21] J. Wang, Z.Q. Lin, Chem. Mater. 20 (2008) 1257.
[22] A. Ghicov, S.P. Albu, J.M. Macak, P. Schmuki, Small 4 (2008) 1063.
[23] C.J. Lin, Y.H. Yu, Y.H. Liou, Appl. Catal. B 93 (2009) 119.
[24] J.R. Jennings, A. Ghicov, L.M. Peter, P. Schmuki, A.B. Walker, J. Am. Chem. Soc. 130 (2008) 13364.
[25] Y. Jo, I. Jung, I. Lee, J. Choi, Y. Tak, Electrochem. Commun. 12 (2010) 616.
[26] C.A. Grimes, G.K. Mor, TiO_2 Nanotube Arrays: Synthesis, Properties, and Applications, Springer, 2009, pp. 30–34, Chapter 1.
[27] J.M. Macak, S.P. Albu, P. Schmuki, Phys, Stat. Sol. (RRL) 1 (2007) 181.
[28] J.M. Macak, S. Aldabergerova, A. Ghicov, P. Schmuki, Phys. Stat. Sol. A 203 (2006) R67.
[29] H.T. Fang, M. Liu, D.W. Wang, T. Sun, D.S. Guan, F. Li, J.G. Zhou, T.K. Sham, H.M. Cheng, Nanotechnology 20 (2009) 225701.
[30] S.P. Albu, A. Ghicov, S. Aldabergenova, P. Drechsel, D. LeClere, G.E. Thompson, J.M. Macak, P. Schmuki, Adv. Mater. 20 (2008) 4135.